Spontaneous emission in GaN/InGaN photonic crystal nanopillars

Aurélien David, Henri Benisty, Claude Weisbuch

Spontaneous emission in GaN/InGaN photonic crystal nanopillars

Aurelien David,[1,2,*] **Henri Benisty,**[1] **and Claude Weisbuch**[2]

[1]*Laboratoire Charles Fabry de l'Institut d'Optique, Campus Polytechnique, Palaiseau, France*
[2]*Materials Department, University of California, Santa Barbara CA, USA*
[*]*Corresponding author: aurelien.david@polytechnique.org*

Abstract: We investigate the physics of spontaneous emission in a photonic crystal (PhC) made of GaN rods with embedded InGaN quantum wells, formed on a thick GaN layer. Although the PhC lies on a higher-index medium, we evidence the existence of unexpected quasi-guided Bloch modes which are strongly localized in the PhC region and possess a long lifetime. These modes determine the behavior of spontaneous emission such as the emission diagram and Purcell effect, as would happen in the usual case of emission in a PhC membrane.

OCIS codes: (230.5298) Photonic crystals; (130.5990) Semiconductors.

References and links

1. P. Lodahl, A. F. van Driel, I. S. Nikolaev, A. Irman, K. Overgaag, D. L. Vanmaekelbergh, and W. L. Vos, "Controlling the dynamics of spontaneous emission from quantum dots by photonic crystals," Nature **430,** 654-657, 2004.
2. M. Fujita, S. Takahashi, Y. Tanaka, T. Asano, and S. Noda, "Simultaneous inhibition and redistribution of spontaneous light emission in photonic crystals," Science **308,** 1296-1298, 2005.
3. D. Englund, D. Fattal, E. Waks, G. Solomon, B. Zhang, T. Nakaoka, Y. Arakawa, Y. Yamamoto, and J. Vuckovic, "Controlling the spontaneous emission rate of single quantum dots in a two-dimensional photonic crystal," Phys. Rev. Lett. **95,** 013904, 2005.
4. E. Viasnoff-Schwoob, C. Weisbuch, H. Benisty, S. Olivier, S. Varoutsis, I. Robert-Philip, R. Houdre, and C. J. M. Smith, "Spontaneous emission enhancement of quantum dots in a photonic crystal wire," Phys. Rev. Lett **95,** 183901, 2005.
5. M. Kitamura, S. Iwamoto, and Y. Arakawa, "Enhanced light emission from an organic photonic crystal with a nanocavity," Appl. Phys. Lett. **87,** 151119, 2005.
6. J. J. Wierer, M. R. Krames, J. E. Epler, N. F. Gardner, M. G. Craford, J. R. Wendt, J. A. Simmons, and M. M. Sigalas, "InGaN/GaN quantum-well heterostructure light-emitting diodes employing photonic crystal structures," Appl. Phys. Lett. **84,** 3885-3887, 2004.
7. T. N. Oder, K. H. Kim, J. Y. Lin, and H. X. Jiang, "III-nitride blue and ultraviolet photonic crystal light emitting diodes," Appl. Phys. Lett. **84,** 466-468, 2004.
8. A. David, T. Fujii, R. Sharma, K. McGroddy, S. Nakamura, S. P. DenBaars, E. L. Hu, C. Weisbuch, and H. Benisty, "Photonic-crystal GaN light-emitting diodes with tailored guided modes distribution," Appl. Phys. Lett. **88,** 061124, 2006.
9. S. Keller, C. Schaake, N. A. Fichtenbaum, C. J. Neufeld, Y. Wu, K. McGroddy, A. David, S. P. DenBaars, C. Weisbuch, J. S. Speck, and U. K. Mishra, "Optical and structural properties of GaN nanopillar and nanostripe arrays with embedded InGaN/GaN multi-quantum wells," J. Appl. Phys. **10,0** 054314, 2006.
10. D. M. Whittaker and I. S. Culshaw, "Scattering-matrix treatment of patterned multilayer photonic structures," Phys. Rev. B **60,** 2610-2618, 1999.
11. H. Rigneault, F. Lemarchand, and A. Sentenac, "Dipole radiation into grating structures," J. Opt. Soc. Am. A **17,** 1048-1058, 2000.
12. D. Delbeke, P. Bienstman, R. Bockstaele, and R. Baets, "Rigorous electromagnetic analysis of dipole emission in periodically corrugated layers: the grating-assisted resonant-cavity light-emitting diode," J. Opt. Soc. Am. A **19,** 871-880, 2002.

#85052 - $15.00 USD Received 9 Jul 2007; revised 26 Oct 2007; accepted 26 Oct 2007; published 18 Dec 2007

13. D. Gerace and L. C. Andreani, "Quantum theory of exciton-photon coupling in photonic crystal slabs with embedded quantum wells," Phys. Rev. B **75,** 235325, 2007.
14. R. R. Chance, A. Prock, and R. Silbey, "Lifetime of an emitting molecule near a partially reflecting surface," J. Chemical Phys. **60,** 2744-2748, 1974.
15. J. P. Dowling and C. M. Bowden, "Atomic emission rates in inhomogeneous-media with applications to photonic band structures," Phys. Rev. A **46,** 612-622, 1992.
16. J. P. Wittke, "Spontaneous emission-rate alteration by dielectric and other waveguiding structures," RCA Review **36,** 655-666, 1975.
17. M. Boroditsky, R. Vrijen, T. F. Krauss, R. Coccioli, R. Bhat, and E. Yablonovitch, "Spontaneous emission extraction and Purcell enhancement from thin-film 2-d photonic crystals," J. Lightwave Technol. **17,** 2096-2112, 1999.
18. P. S. J. Russell, S. Tredwell, and P. J. Roberts, Full photonic bandgaps and spontaneous emission control in 1d multilayer dielectric structures," Opt. Commun. **160,** 66-71, 1999.
19. S. G. Tikhodeev, A. L. Yablonskii, E. A. Muljarov, N. A. Gippius, and T. Ishihara, "Quasiguided modes and optical properties of photonic crystal slabs," Phys. Rev. B **66,** 045102, 2002.
20. J. M. Pottage, E. Silvestre, and P. S. Russell, "Vertical-cavity surface-emitting resonances in photonic crystal films," J. Opt. Soc. Am. A **18,** 442-447, 2001.
21. A. David, C. Meier, R. Sharma, F. S. Diana, S. P. DenBaars, E. Hu, S. Nakamura, C. Weisbuch, and H. Benisty, "Photonic bands in two-dimensionally patterned multimode GaN waveguides for light extraction," Appl. Phys. Lett. **87,** 101107, 2005.
22. S. Mathias, M. Wiesenmayer, M. Aeschlimann, and M. Bauer, "Quantum-well wave-function localization and the electron-phonon interaction in thin Ag nanofilms," Phys. Rev. Lett. **9,7** 236809, 2006.
23. N. Koide and K. Ujihara, "Analysis of spontaneous emission from a planar microcavity dependence on the refractive-index of the cavity region and atomic location," Opt. Commun. **111,** 381-393, 1994.

1. Introduction

Spontaneous emission in the presence of a light confining structure has been extensively studied in photonic crystals (PhCs),[1, 2, 3, 4, 5] notably in the case of emission in a PhC membrane displaying a photonic band gap and its derived structures (defect cavities or waveguides created by missing holes in such membranes). Membranes provide a "textbook" system where efficient light confinement is obtained by the PhC and by refractive index guiding in the vertical direction. Periodic membranes as well as point and line defects have been studied in this respect. For real-world device applications however, current injection is necessary and leads to less ideal structures. In the field of high-efficiency light emitters for instance, PhCs can be considered for enhanced light extraction in a geometry where the substrate is retained.

GaN-based materials constitute an important material for solid-state light emitters, and numerous implementations of PhC-assisted light emitting diodes have been demonstrated [6, 7, 8]. Etch-induced damage to the material remains a concern in this case as it can scavenge carriers and spoil the overall efficiency. However, Keller *et al.* recently demonstrated that suitable annealing can heal such damage, even when the PhC is etched *through* the InGaN active region [9]. The resulting structure is rather unusual: it consists of a GaN/air PhC lying on a thick GaN buffer, grown on a sapphire substrate. In this case, one can expect rather strong effects on spontaneous emission because the source is embedded in the PhC. On the other hand, the absence of vertical index confinement makes the modal distribution much more complex so that it is challenging to predict trends for the amount of overall light extraction enhancement.

In this article, we explore some properties of spontaneous emission in such structures. In particular, we show that confinement in the vertical direction is more effective than could be anticipated, making it clear that part of the underlying physics is two-dimensional, while providing a clear extraction enhancement in the vertical (third) direction.

2. Light emission in PhC membranes

In this section, we first briefly review the well-known case of spontaneous emission in a monomode PhC membrane. This simple situation will serve as a basis for the analysis of emis-

#85052 - $15.00 USD Received 9 Jul 2007; revised 26 Oct 2007; accepted 26 Oct 2007; published 18 Dec 2007

sion diagrams in more complex structures. This will be justified by our final findings, namely that emission in the structure of interest retains a strong two-dimensional character.

2.1. *Low-frequency behavior*

In a textured membrane, a first heuristic regime occurs at low frequencies, where the reciprocal lattice vectors **G** are so large compared to $k_{//} = \langle n \rangle \omega/c$ ($\langle n \rangle$ being an average membrane effective index) that they cannot bring guided modes into the small air cone $k_{//} = \omega/c$. Hence, guided modes undergo the photonic crystal perturbation on their own, while direct emission to the air is essentially unchanged – or only perturbatively affected. We shall first discuss in the following the emission in this regime to enlighten the distinctive features of vertical confinement and in-plane structure of a photonic crystal membrane.

Let us consider a symmetric, monomode PhC membrane possessing a band gap for TE in-plane polarization. In this work, we will consider light emitters which are delocalized in the horizontal direction, such as excitons in a quantum well - this is in contrast to the usual point dipole sources used to model quantum dot emitters. The reason for this is twofold: we are interested in InGaN/GaN quantum wells, and the delocalized nature of excitons saves us from dealing with the emitter's in-plane location in the PhC, thus simplifying the discussion. [1]

As mentioned above, spontaneous emission can occur through two well-separated channels: light which is directly propagative in air (corresponding to wavevectors $k_{\|} < k_0$) and guided light in the fundamental TE mode.[2] Therefore, the Purcell factor can be written as:

$$F_p = F_{air} + F_{guided} \tag{1}$$

Where F_{air} and F_{guided} are the Purcell factors to air and to the guided modes. Each Purcell factor represents the modification of the photonic density of states (DOS) in the corresponding channel, with respect to the free-space value (Refs. [14, 15, 16, 17] see also Ref. [18] for a source in a low-index medium):

$$F_{guided} = \frac{\rho_{guided}}{\rho_0} = \frac{\rho_{guided}}{\omega^2 n^2 8\pi/3} \tag{2}$$

Where:

$$\rho_{guided}(\omega) = \sum_n \int_{Sn} \frac{dk_{\|}}{|\nabla\omega|} |\mathbf{d}.\mathbf{A}_n|^2 \tag{3}$$

The sum index n runs over the guided modes of the membrane, and each integral is taken over the fermi surface S_n of the corresponding guided mode, **d** is the dipole moment and $\mathbf{A}_n$ the vector potential of the guided mode. In the present case, there is only one TE guided mode.

In the vicinity of the photonic gap, the DOS of air modes (ρ_{air}) undergoes weak variations while the guided DOS (ρ_{guided}) is strongly affected by the term $\nabla\omega$. Therefore, taking the air DOS as constant, the Purcell factor takes the simple form:

$$F_p = \frac{3}{8\pi\omega^2 n^2} \left(\rho_{air} + \rho_{guided}(\omega)\right) \tag{4}$$

[1] More precisely, we consider sets of in-plane dipole forming a dipole sheet , each elementary dipole corresponding to an exciton and emitting *incoherently* at a given $k_{\|}$. Because of this incoherent sum, the dipole moment is modeled as $\mathbf{p}exp(i\mathbf{k}_{\|}\cdot\mathbf{r})$ rather than $\mathbf{p}\sum_G exp(i(\mathbf{k}_{\|}+\mathbf{G})\cdot\mathbf{r})$ as in Refs. [10, 11, 12]. A more rigorous discussion of the quantization of excitons in a PhC can be found in Ref. [13]

[2] A TM mode is also present, but for the case we consider (a dipole sheet with in-plane polarization located at the center of a symmetric membrane) no light is emitted in this mode for symmetry reasons, which simplifies our discussion.

#85052 - $15.00 USD Received 9 Jul 2007; revised 26 Oct 2007; accepted 26 Oct 2007; published 18 Dec 2007

For illustration, we consider a GaN ($n = 2.5$) membrane of thickness $0.5a$ etched by a triangular lattice PhC (lattice constant a, filling factor $f = 0.4$). The band structure of the TE guided mode and the corresponding guided DOS, computed by the RCWA method [19], are shown in Fig. 1.

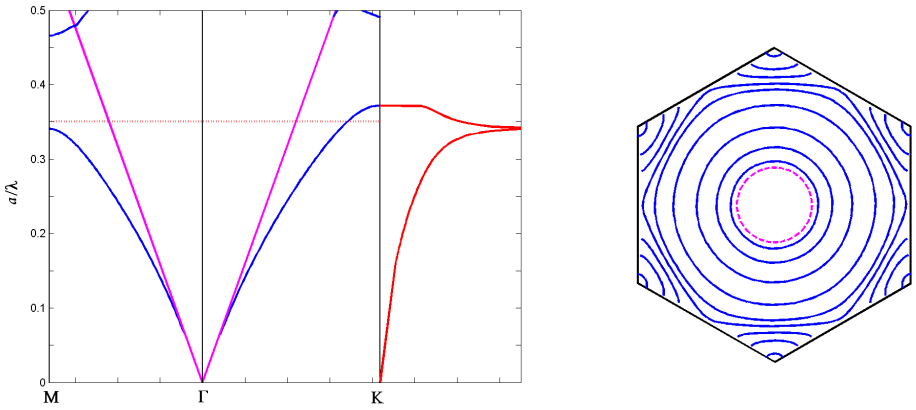

Fig. 1. (Left) Band structure of a GaN PhC membrane. Blue: band structure of the fundamental TE Bloch mode. Red: Corresponding DOS ρ_{guided}. Magenta: air cone. (Right) Corresponding Fermi surfaces at frequencies a/λ=0.15, 0.2, 0.25, 0.3, 0.33, 0.34, 0.35, 0.36, 0.37 (from center to edge of the reduced Brillouin zone). Magenta dashed circle: air cone.

As can be seen, the guided DOS shows a peak close to the gap at the M point: this logarithmic singularity corresponds to a photonic version of the Van Hove singularity. When approaching the gap at the K point, ρ_{guided} tends to a constant value before vanishing at the gap frequency u_{gap}. Indeed, close to the K point the dispersion is parabolic, yielding a constant DOS according to Eq. 3 – in the same way as usual electronic quantum wells whose dispersion relation reads $E(\mathbf{k}) \sim \mathrm{k}^2$ around a singular point of k-space (usually the Γ point).

To confirm this simple approach to spontaneous emission, we compute the emission diagram [10, 11, 12] for a light source at various frequencies around the gap (Fig. 2). Each diagram is normalized [12], so that integration over its full surface yields the total Purcell factor F_p. The partial Purcell factors F_{air} and F_{guided} are thus obtained by integrating the emission diagrams inside and outside the light cone respectively.

As can be seen, F_{guided} follows ρ_{guided} while F_{air} remains roughly constant. Figure 2 also details the emission diagram at $u = 0.35$, close to the gap at point K. Light emission occurs into the continuum of modes in air and into the Bloch modes, whose isofrequency contours form, as expected, small rounded triangles around the K points. These triangles eventually change to circles even closer to the K gap.

From this discussion, we conclude that the properties of a light source in a PhC membrane are mainly dictated by coupling to the corresponding Bloch mode. This also shows up in the emission diagram of the source, which follows the Fermi surface of the Bloch mode. This trend is valid because we look at "monomode" guidance in the vertical direction so that the z-profile of the mode is not an issue – the dipole overlap with the mode profile $\mathbf{A}$ is close to constant.

2.2. Higher frequency behavior

Let us now discuss the extension to higher frequencies, focusing on extraction of Bloch modes to air. The reciprocal lattice vectors $\mathbf{G}$ are now of the same order as $k_{//} = \langle n \rangle \omega/c$, so that Bloch

#85052 - $15.00 USD Received 9 Jul 2007; revised 26 Oct 2007; accepted 26 Oct 2007; published 18 Dec 2007

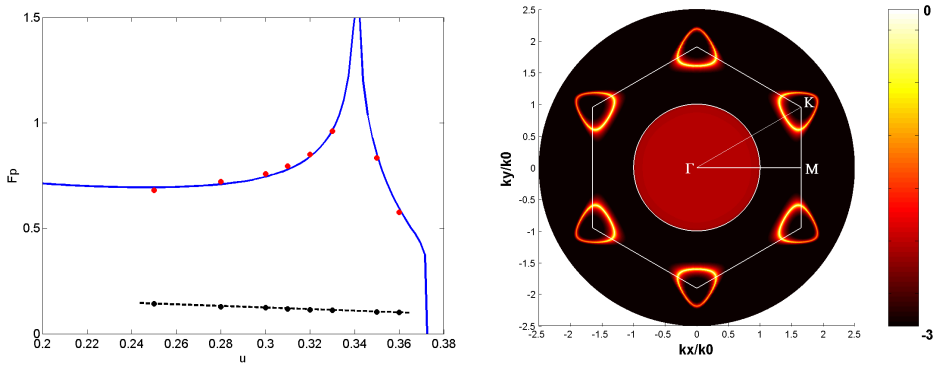

Fig. 2. (Left) Red dots: Purcell factor F_{guided} for the guided Bloch mode. Blue line: ρ_{guided}/ω^2 (the guided DOS normalized by the frequency) is seen to coincide with the Purcell factor in this simple case. Black dots: Purcell factor F_{air} for emission to air - emission in the air continuum is nearly constant and not affected by the PhC (the dashed black line is a guide to the eye). Note that the total Purcell factor $F_{guided} + F_air$ is usually smaller than one (except close enough to the Van Hove singularity). This is because the calculation is normalized to $F_p = 1$ for emission in bulk GaN, and on average the dipole in the membrane "feels" a dielectric with an index lower than that of bulk GaN. (Right) Emission diagram of a quantum well in a GaN PhC membrane, at a frequency $u = 0.35$. This diagram displays the power emitted (in log scale) as a function of direction. k_x and k_y are the components of the in-plane wavevector of photons in units of k_0. The white circle is the air cone, and the white hexagon the first Brillouin Zone. The emission diagram is composed of direct emission into the air continuum, and of emission into the Bloch mode following the mode's isofrequencies.

modes can now be folded well inside the first Brillouin zone and become leaky modes which are extracted to air. Conversely the air cone $k_{//} = \omega/c$ can approach the boundaries of the first Brillouin zone or even exceed them. The result is that the previously smooth continuum of air modes is now scarred with grating anomalies (or Wood anomalies) due to guided modes.[20] These possibly strong scars in the continuum of air modes make the situation more complex. However, Bloch modes retain a well-defined isofrequency wavevector locus in spite of this coupling.

The precise isofrequency shapes which can be expected for a Bloch mode above the fundamental gap are depicted qualitatively in a free-photon picture (assuming a Bloch mode with effective index $n_{eff} = 1.6$) in Fig. 3. Let us detail the behavior of this generic dispersion relation. Extraction of the Bloch mode to air along ΓM arises just above the red frequency line (at $a/\lambda \sim 0.42$). At this stage, the isofrequency contours are made of circles which form small triangles around K points (Fig. 3b). The apexes of the triangles are however inverted with respect to those of Fig. 2 because we are now in the air band rather than the dielectric band. A trend of constant photonic DOS is also manifested in this region, by the same argument as for the top of the dielectric band.

As the frequency grows, so do these rounded triangles. Importantly, the light circle also grows with frequency. In this intermediate case (green line on Fig. 3) some fraction of the rounded triangles is extracted to air, but another part is still in the uncoupled area. At a frequency $\sim a/\lambda = 1/\sqrt{3} = 0.58$ (blue line) the light circle touches the Brillouin zone edge. This means that the only non-extracted areas are those around K points. Fortunately, the rounded triangles now tend to be large enough to approach the M points and avoid K points: they are then always

#85052 - $15.00 USD Received 9 Jul 2007; revised 26 Oct 2007; accepted 26 Oct 2007; published 18 Dec 2007

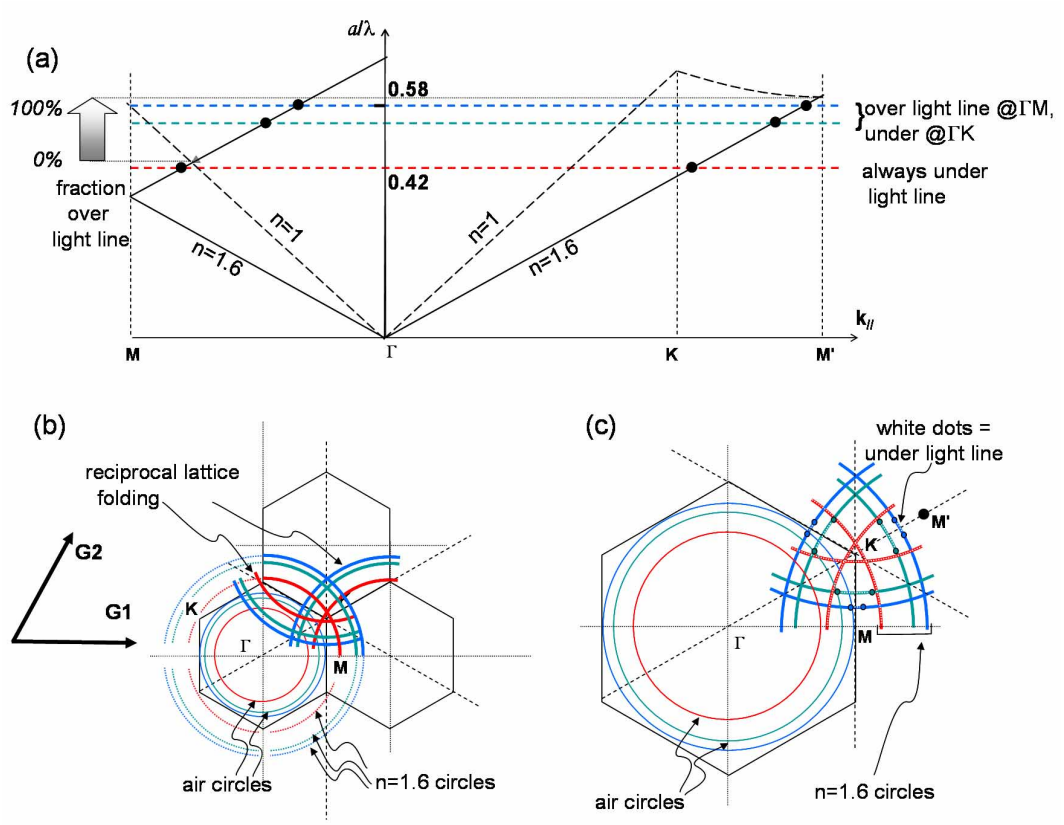

Fig. 3. (a) Generic quasi-free photon band structure along ΓM and ΓKM' for photons of effective index $n_{eff} = 1.6$. Diffraction to air first becomes possible along ΓM around a frequency $u = 0.42$ (red dashed line). At higher frequencies $u = 0.54$ and $u = 0.58$ (green and blue dashed lines respectively) a larger part of the band structure is located above the light line. (b) Corresponding isofrequencies and air cones for these three frequencies (red $u = 0.42$, green $u = 0.54$, blue $u = 0.58$). The "$n = 1.6$" circles are the isofrequencies (i.e. wavevector locus) for $n_{eff} = 1.6$, and their foldings by the reciprocal lattice. The air circles correspond to $n_{eff} = 1$. Diffraction is possible when an isofrequency is folded inside the corresponding air circle. (c) Zoom on (b) detailing the fate of the mode: the red frequency is never extracted, the green frequency is partly unextracted. The blue frequency is almost completely extracted, while keeping the air-circle at the smallest possible diameter.

extracted.

Let us however comment on the nature of this extraction process: we are dealing with a guided mode decorated by Bloch harmonics, but whose main harmonic – carrying most of the power – is the actual guided mode (corresponding to the circle centered around Γ on Figure 3b). Thus in practice, the near perfect theoretical light extraction has to be weighted by the strength of the outcoupling versus other experimentally competing photon scavenging processes (scattering, absorption...).

Again, we illustrate this qualitative description with a numerical simulation. We consider here a GaN membrane of thickness a etched by a triangular lattice PhC (lattice constant a, filling factor $f = 0.5$). Figure 4 presents the emission diagram of a source located in the middle of this membrane, at a frequency $u = 0.6$.

#85052 - $15.00 USD Received 9 Jul 2007; revised 26 Oct 2007; accepted 26 Oct 2007; published 18 Dec 2007

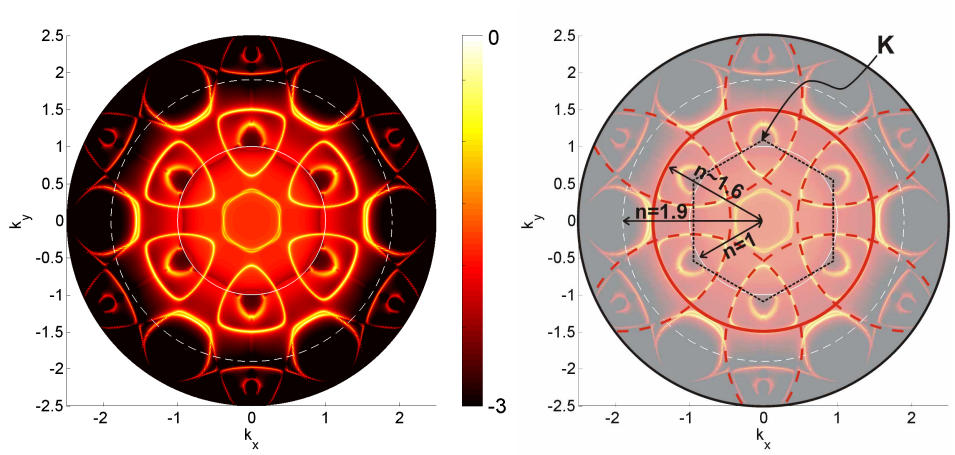

Fig. 4. PhC membrane emission diagram. (Left) Emission diagram of a quantum well in a GaN PhC membrane (the emitted power is in log scale, k_x and k_y in units of k_0). The small full circle is the air cone ($n = 1$), and the large dashed circle corresponds to the average index of the membrane ($n_{eff} = 1.9$): emission is strongly suppressed beyond this circle. The sharp features correspond to emission in Bloch modes. (Right) Emission diagram with the isofrequency contours of a free-photon mode ($n_{eff} = 1.6$) superimposed as red lines. The full red circle is the dispersion of a guided mode with $n_{eff} = 1.6$, and the dashed circles correspond to periodization by the reciprocal lattice, e.g. to the harmonics of the Bloch mode.

The main characteristics of the emission diagram correspond to the above discussion. One can still distinguish a background of emission into the air continuum, and sharp features corresponding to the Bloch mode. We note that emission into the air continuum now extends beyond the air cone: this is because the grating allows outcoupling of light with $k_{parallel} > k_0$ to the continuum. The Bloch mode's dispersion is close to that of a free photon with $n_{eff} = 1.6$, and we observe the expected rounded triangles around the K points. However, photonic interaction between the harmonics opens anticrossings (e.g. mini-stop bands) in the free photon dispersion so that some parts of the folded circles vanish.

This closes our discussion of emission in a PhC membrane.

3. Light emission diagram in partially-etched multimode structures

Let us now come to a more realistic structure: a sapphire substrate ($n = 1.7$), a 1μm thick GaN layer, a 400nm thick PhC (triangular lattice of circular *GaN rods in an air matrix*, with a filling factor $f = 0.5$ and a period a=200nm), and an air superstrate. We consider a reduced frequency $u = 0.58$. Investigation of such a structure is prompted by the recent reports of efficient luminescence of similar, partially-etched GaN/InGaN samples (Ref. [9]).

In contrast to the simple case of the previous section, the radiative channels available for spontaneous emission are now less obvious. Clearly, the continuum of "air modes" must still be present - as well as a continuum of modes in the sapphire substrate. In addition, the unetched region of the GaN layer constitutes a thick waveguide supporting numerous Bloch modes - which can be propagative or evanescent in the PhC region, depending on their effective index n_{eff}. Such Bloch modes were observed experimentally in Ref. [21]. Figure 5 sketches this tentative distribution of radiative channels. Intuitively, one may argue that light emission will be broadly averaged over these numerous channels.

#85052 - $15.00 USD Received 9 Jul 2007; revised 26 Oct 2007; accepted 26 Oct 2007; published 18 Dec 2007

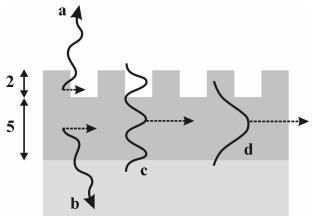

Fig. 5. Radiative channels in the structure. Dashed arrows: corresponding in-plane wavevectors $k_{||}$. (a) Continuum of air modes, with $k_{||} < k_0$ (b) Continuum of sapphire modes with $k_{||} < n_{sapphire} k_0$ (c) Bloch mode propagative in the GaN and PhC region (d) Bloch mode of larger $k_{||}$, evanescent in the PhC region.

In contrast to this intuitive view, Fig. 6 displays the result of an emission diagram calculation in such a structure: it appears that most of the light emission actually occurs in a strongly peaked, "egg-shaped" feature. This feature clearly possesses a dispersion reminiscent of the Fermi surfaces described in the previous section. It is localized around the *K* points, which is indicative of partial band gaps around the *M* directions. The intensity of this feature in the emission diagram suggests the existence of a strong resonance in the PhC region, located around a gap at the K point. In addition, the sharpness of this resonance manifests its rather long lifetime.

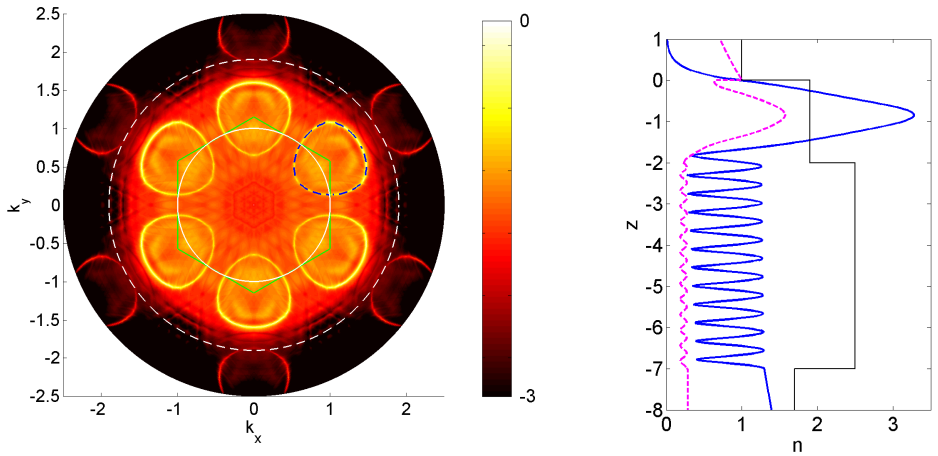

Fig. 6. (Left) Emission diagram for $z_s = 1.45$. The green lines correspond to the boundary of the first Brillouin zone. The isofrequency of the Bloch mode localized in the PhC region is superimposed as a blue dashed line: it follows exactly the emission peak of the diagram. (Right) Modulus of the electric field ($|E|$) along z for the localized Bloch mode, in the ΓK direction. Blue line: fundamental harmonic. Magenta line: second-largest harmonic. The average index profile is represented by the black line.

This resonance can actually be computed directly as a Bloch mode of the structure, provided one allows proper (leaky) boundary conditions. The result of this calculation is shown on Fig. 6. As expected, the Fermi surface of this mode precisely follows the sharp feature of the emission diagram. Quite surprisingly, the mode is strongly localized vertically in the PhC region of the structure (Fig. 6) - although this region lies on a GaN layer of *higher* index.

#85052 - $15.00 USD Received 9 Jul 2007; revised 26 Oct 2007; accepted 26 Oct 2007; published 18 Dec 2007

Another unexpected element is the lifetime of this mode. Its wavevector (along ΓK) is $k_{\parallel} \sim 6 + 0.02i$. This corresponds to an effective index $n_{eff} \sim 1.6$, smaller even than the index of sapphire: therefore, one could expect this mode to spread within the GaN buffer layer and leak quickly to the sapphire substrate. In contradiction with this view, the imaginary part of $k_{\parallel}$ is rather low: it corresponds to a decay length $L_{decay} \sim 20a$, indicating that the mode spends a rather long time in the PhC region before leaking to the GaN and sapphire. Let us stress that we are considering the effective index associated with the *fundamental* harmonic ($\mathbf{G} = 0$) of the mode, which carries most of its power. Typically for a leaky mode, other harmonics cause moderate diffraction losses and have a small n_{eff}. However, the current mode is unexpected because it has a long lifetime, although even the fundamental harmonic can leak to the substrate.

Let us now study the mechanisms responsible for the existence of this atypical mode.

4. Quasi-guided Bloch modes in PhC without vertical index confinement

4.1. Quasi-guided modes in a low index layer

To understand the origin of this Bloch mode, let us first come back to the very simple case of a low-index (n_1) layer sandwiched between air and a high-index (n_2) material. Of course, the layer does not support any guided mode. However, let us consider a light beam propagating at a given angle θ inside the layer (above the critical angle with air for simplicity): this beam undergoes total reflection at the air interface, and partial Fresnel reflection with coefficient r at the low/high index interface. If θ is large enough, r can be close to 1 and the beam can bounce many times before leaking to the high index material. Thus, we are led to introduce *quasi-guided modes* (QGM) in the low-index layer. The resonance condition is fulfilled when the phase of the beam is matched after a round trip in the layer. If we denote as $k_{\parallel 1D}$ and k_z the in-plane and vertical wavevectors of the mode, this corresponds to: [3]

$$k_z = \frac{\pi}{L} \tag{5}$$

This imposes the following values for $k_{\parallel}$ and θ:

$$k_{\parallel 1D} = \sqrt{n_1^2 k_0^2 - (\pi/L)^2} \quad , \quad cos\theta = \frac{1}{2Ln_1 u} \tag{6}$$

In a round-trip in the PhC layer, light travels a distance $2Ltan\theta_1$ in the x direction and the amplitude loss is $(1-r)$, which yields the following imaginary part for the in-plane wavevector:

$$k'' = -\frac{ln(-r)}{2Ltan\theta} \tag{7}$$

k'' vanishes as $\theta \to \pi/2$, both because $r \to 1$ and because the beam travels a larger distance before impinging on the interface.

To illustrate this, let us consider a layer of thickness 2 and index 1.9, sandwiched between air and a substrate of index 2.5 – this corresponds to our earlier structure, where the PhC is replaced by a homogeneous layer with the same average index (Fig. 7). According to Eqs.(6-7) this layer supports a QGM propagating at an angle $\theta = 77^o$ and with a loss rate $k'' = 0.027$. A numerical solution of the Helmholtz equation in the structure confirms the existence of this resonance and yields $\theta = 78^o$ and $k'' = 0.025$, thus supporting our description of this QGM. Let us note that the low loss of the QGM is made possible by its nearly-glancing angle of propagation – or equivalently, by its high effective index: $n_{eff} = 1.86$, very close to the index of the layer $n = 1.9$.

[3] The beam also undergoes a phase shift of π at the low/high index interface, and another phase shift at the low index/air interface which is very close to π for such glancing angles. The resulting 2π shift therefore cancels out.

#85052 - $15.00 USD Received 9 Jul 2007; revised 26 Oct 2007; accepted 26 Oct 2007; published 18 Dec 2007

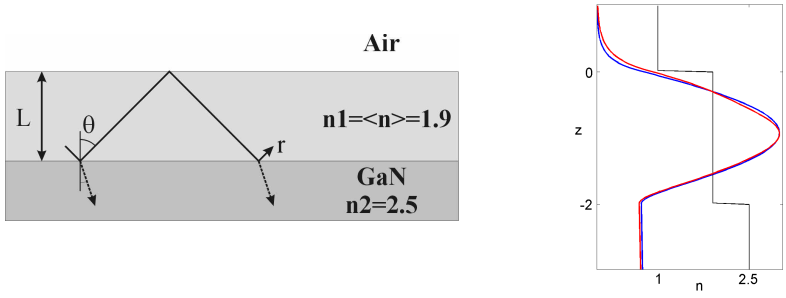

Fig. 7. (Left) Geometry of the structure. (Right) Blue line: profile of the electric field $|E|$ of the 1D QGM (with $n_{eff} = 1.86$), obtained by solving numerically the Helmholtz equation. Red line: $|E|$ for the fundamental harmonic of corresponding Bloch QGM (taking scattering by the PhC into account), propagating with $n_{eff} = 1.6$. The profile of both modes is nearly identical despite the difference in effective index, evidencing that the mode's profile is imposed by phase matching in the vertical direction.

This resonance is the basis on which the Bloch mode observed earlier is built. It is a simple Fabry-Perot resonance, but whose large propagation angle yields a very low loss. Although such resonances have attracted little attention in the past, they can readily be observed experimentally, for instance when light is emitted inside a low-index material on a high index substrate. Let us also note that analogous electronic resonances have been investigated recently in Ag quantum wells, and are characterized by an energy above the quantum well barrier.[22]

4.2. Quasi-guided Bloch modes in a periodic low index layer

Let us now investigate the effect of periodicity on such a QGM. To this effect, we use a simple coupled-wave model with two waves, where a 1D QGM E^+ can couple to a counter-propagating harmonic E^- through a reciprocal vector G. In this simple case, Maxwell's equations become:[4]

$$\omega^2 \begin{pmatrix} \varepsilon_0 & \varepsilon_1 \\ \varepsilon_1 & \varepsilon_0 \end{pmatrix} \begin{vmatrix} E^+ \\ E^- \end{vmatrix} = \begin{vmatrix} k_\parallel^2 + k_z^2 \\ (k_\parallel - G)^2 + k_z^2 \end{vmatrix} \cdot \begin{vmatrix} E^+ \\ E^- \end{vmatrix} \tag{8}$$

Here, ε_0 is the dielectric constant of the propagation medium, $k_\parallel$ and k_z are the in-plane and vertical wavevectors of the mode. G is the reciprocal vector coupling the waves, and ε_1 the strength of the coupling.

This system can of course be solved numerically. Let us also look for an analytical solution. We call $k_{\parallel 1D}$ the in-plane wavevector in the absence of coupling (given by Eq. 6), and $k_\parallel = G/2 + K$ the in-plane wavevector in the presence of coupling. To obtain a simple analytical solution, let us assume that, at a given frequency, the vertical wavevector k_z is still imposed by the phase matching condition and is therefore unchanged by the presence of the coupling, i.e.:

$$k_z^2 = \varepsilon_0 \omega^2 - k_{\parallel 1D}^2 \tag{9}$$

The vertical profiles of the guided and Bloch QGM are compared on Fig. 7: they are nearly similar, supporting this hypothesis. The solution of Eq. 8 under this assumption is:

[4]With $c = 1$, implying $\omega = k_0 = 2\pi/\lambda$.

#85052 - $15.00 USD Received 9 Jul 2007; revised 26 Oct 2007; accepted 26 Oct 2007; published 18 Dec 2007

$$K^2 = \frac{G^2 + 2(k_{\parallel 1D}^2 - G^2/4) - \sqrt{\left(G^2 + 2(k_{\parallel 1D}^2 - G^2/4)\right)^2 + 4\omega^4\varepsilon_1^2 - 4(k_{\parallel 1D}^2 - G^2/4)^2}}{2} \tag{10}$$

To study the properties of Eq. 10, let us neglect the small losses of the mode and assume that $k_{\parallel 1D}$ is real. In this case, we are dealing with a simple second-order equation with real parameter and three regions of interest appear for the solution K^2:

$$\begin{aligned}
&k_{\parallel 1D}^2 - G^2/4 < -\omega^2|\varepsilon_1| && \rightarrow \quad K^2 > 0, K \in \mathbb{R}, K < 0 \quad \text{(dielectric band)} \\
&-\omega^2|\varepsilon_1| < k_{\parallel 1D}^2 - G^2/4 < \omega^2|\varepsilon_1| && \rightarrow \quad K^2 < 0, K \in i\mathbb{R} \quad \text{(gap)} \\
&\omega^2|\varepsilon_1| < k_{\parallel 1D}^2 - G^2/4 && \rightarrow \quad K^2 > 0, K \in \mathbb{R}, K > 0 \quad \text{(air band)}
\end{aligned} \tag{11}$$

Where the sign of K has been deduced from its asymptotic behavior.[5] We recover the well-known opening of a band gap at $k_\parallel = G/2$. The band located below the band gap is bent 'down', corresponding to a higher effective index (i.e. a stronger localization of the mode in the dielectric) and is therefore termed *dielectric band*. Likewise, the band above the band gap corresponds to localization in the air and is called the *air band*. These results are exemplified on Fig. 8, where the parameters correspond to a PhC membrane of GaN rods in air with $f = 0.5$ and only two coupled waves (air superstrate, GaN substrate).

Notably, it appears that although the coupling significantly modifies the effective index close to the Bragg condition, it has little impact on the loss coefficient (except in the gap region of course) because losses are dominated by the leakage of the fundamental harmonic, whose vertical phase-matching condition (Eq. 9) is not modified by the coupling.

The nature of our quasi-guided Bloch mode (QGBM) can thus be understood as follows: the 1-dimensional QGM supported in the low-index region gets preferentially localized in air due to the scattering of the PhC. This lowers its effective index, while keeping the loss coefficient low. The resulting Bloch mode thus displays low losses at an 'anomalously low' effective index, i.e. in spite of its ability to leak in the GaN buffer and the sapphire substrate.

Let us note that, while we ignored the presence of the sapphire substrate when justifying the existence of this mode, our arguments still hold in its presence – although additional small reflections at the GaN/sapphire interface may somehow modify the loss coefficient of the mode.

5. Purcell effect and emission distribution in partially-etched multimode structures

Having accounted for the existence of this atypical QGBM, we now come back to the structure under investigation and study spontaneous emission in more details. Figure 9 displays the Purcell factor of a light source as a function of its vertical position in the structure. For comparison, the Purcell factor in a 1D 'average index' case (e.g. considering the PhC as a homogeneous layer of index $\langle n \rangle = 1.9$) is also indicated.

As can be seen, the actual Purcell factor departs significantly from the 1D approximation when the source is inside the PhC and couples to the PhC modes. Outside of the PhC on the other hand, F_p closely follows the 1D result, indicating that the PhC modes do not alter spontaneous emission significantly.

So far, we only focused on the 'fundamental' QGBM stemming from the fundamental QGM of the 1D structure. However, several QGM can be supported by a low-index layer depending

[5] Namely, $K < 0$ when $\omega \rightarrow 0$ and $K > 0$ when $\omega \rightarrow \infty$.

#85052 - $15.00 USD Received 9 Jul 2007; revised 26 Oct 2007; accepted 26 Oct 2007; published 18 Dec 2007

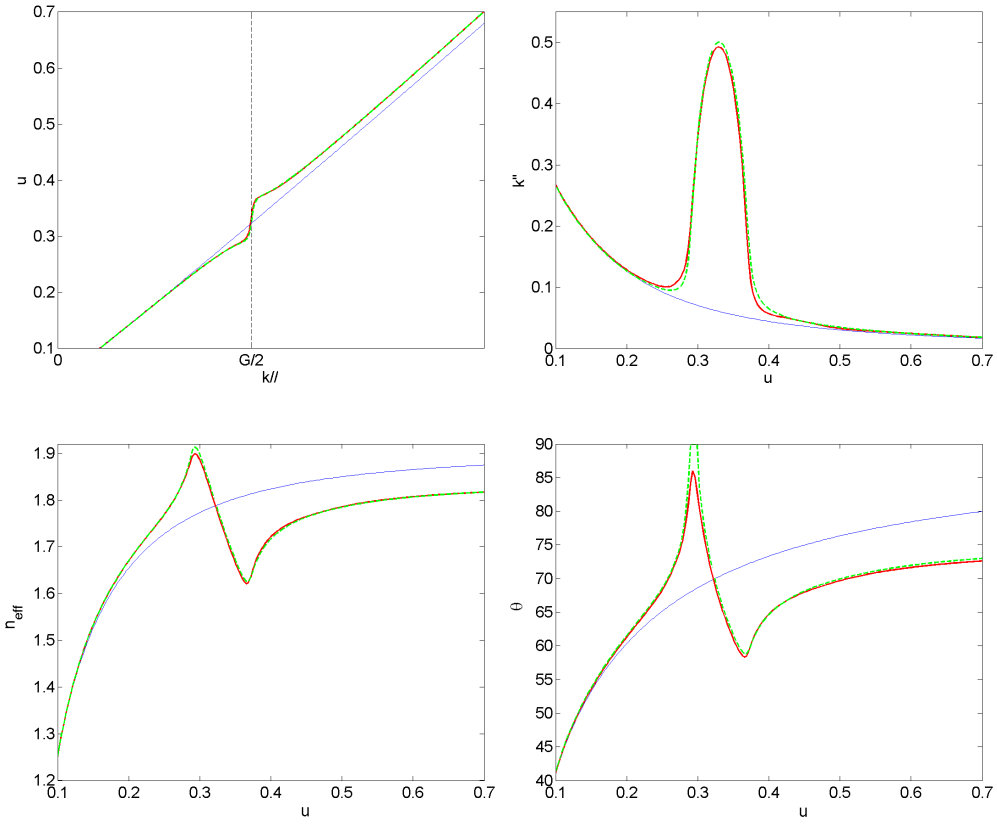

Fig. 8. Propagation properties of the uncoupled 1D QGM (thin blue line), and the coupled QGBM (red thick line: numerical result, green dashed line: analytical solution of Eq 10). As can be seen, the analytical solution is in general very close to the numerical solution. (Top left) Dispersion relation. The coupling causes a gap opening at G/2 (dashed vertical line). (Top right) Loss coefficient k''. In the presence of coupling, k'' is high in the gap due to reflection. Outside of the gap, losses are dictated by the leakage of the fundamental harmonic and barely modified by the coupling. (Bottom left) Effective index n_{eff}. Below the gap, the mode localizes in the dielectric and n_{eff} increases with respect to the 1D value. Above the gap on the other hand, the mode localizes in air and n_{eff} decreases. Notice the *rigid shift* of n_{eff} caused by the coupling at high frequency: its asymptotic value is not $\langle n \rangle$ but $\langle n \rangle \sqrt{1-\varepsilon_1/\langle n \rangle^2}$. (Bottom right) Corresponding angle of propagation.

on its thickness, as sketched on Fig. 10. Their resonance conditions, and the corresponding field profiles, are characterized by:

$$k_z^p = \frac{p\pi}{L}\ ,\ E^p \sim cos(k_z^p z) \tag{12}$$

In our case, four QGBM should be supported by the PhC region (using the cutoff condition $k_0 < k_z < 1.9k_0$). Of course, they are not expected to be as well-defined as the fundamental QGBM (because of their much higher loss coefficient). However, the rather strong oscillations of F_p in Fig. 9 suggest that spontaneous emission is influenced by coupling to these QGBM. [6]

[6]This effect is more pronounced than in the 1D case, where emission to the continua of air and sapphire dominate emission, and the oscillations due to the QGM are weak.

#85052 - $15.00 USD Received 9 Jul 2007; revised 26 Oct 2007; accepted 26 Oct 2007; published 18 Dec 2007

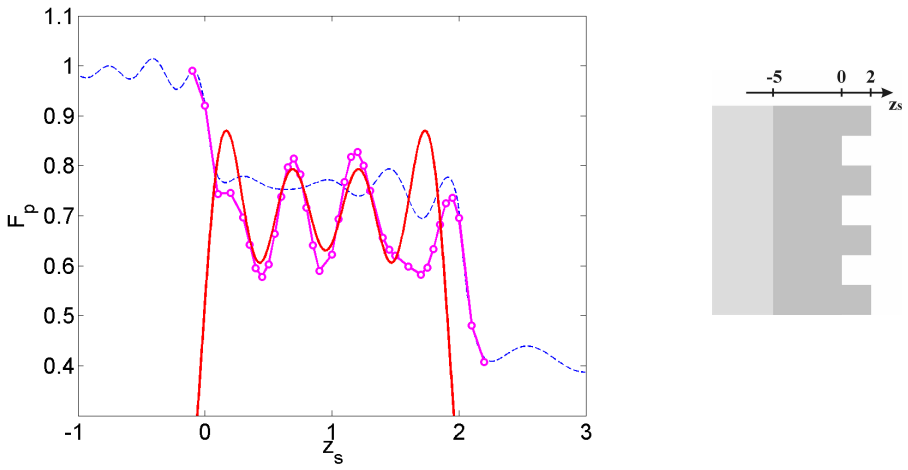

Fig. 9. Purcell factor as a function of the source's position z_s in the structure. Magenta line with dots: actual Purcell factor F_p. The strong oscillations of F_p are due to coupling to the QGBM. Dashed line: 'average index' result. Oscillations of F_p are weak in this approximation, because spontaneous emission is dominated by emission to the sapphire and air continua. Red line: fit by Eq. 13.

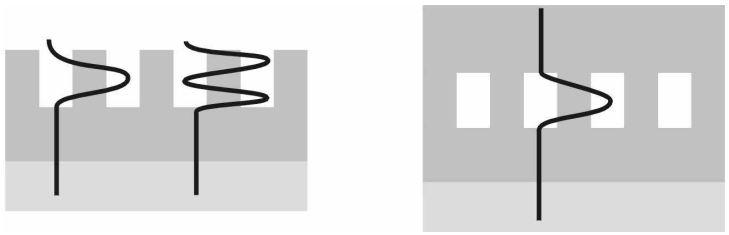

Fig. 10. (Left) Generalization of the QGM to higher-order quasi-guided resonances in the PhC region. Here, the first and second resonances are depicted. (Right) QGM in a GaN/PhC/GaN structure: the mode is trapped in the low-index region, and constitutes an easily injectable photonic crystal membrane.

In order to account for this, we suggest a very simplified approach where the PhC layer is considered as a simple Fabry-Pérot cavity supporting four modes. In this case, the spontaneous emission rate at position z_s in the cavity ins simply proportional to the coupling to each mode[23]:

$$F_p(z_s) \sim \sum_p sin(k_z^p z_s)^2 \tag{13}$$

Figure 9 displays the result of this heuristic approach. Remarkably, the fit is reasonable: the amplitude of the oscillations of F_p are on the right order. This suggests that spontaneous emission is indeed strongly dominated by emission into the four QGBM. The positions of the first and last maxima, however, are not well reproduced: this can be expected since these peaks are due to coupling to the fourth QGBM, for which Eq. 13 is least valid.

#85052 - $15.00 USD Received 9 Jul 2007; revised 26 Oct 2007; accepted 26 Oct 2007; published 18 Dec 2007

6. Conclusion

We have studied the behavior of spontaneous emission in a PhC lying on a high-index substrate. In spite of the apparent lack of vertical confinement, it turns out that such a system still supports Bloch modes which are strongly localized vertically in the PhC. These modes are efficiently coupled to the light source in the PhC and therefore influence the properties of emission such as the emission diagram and the Purcell effect. Their existence and peculiar properties are well explained by a single coupled-wave model starting from a quasi-guided Fabry-Pérot resonance in a 1D multilayer system. Let us stress that, although for a source plane outside of the PhC spontaneous emission is well explained by a 1D model, inside the PhC spontaneous emission is strongly modulated, manifesting a remarkable Bloch wave confinement.

To conclude this article, we give some perspectives on the possible use of such resonance for practical applications. Diffractive filters, for instance, may make use of such a resonance (in contrast to the common view that optical confinement by a substrate is necessary to obtain sharp Fano resonances in a filter, as in Ref. [20]). Besides, the existence of these modes holds even if GaN is present on both sides of the PhC region, instead of an air superstrate (the mode's losses are simply doubled). Such a structure, depicted in Fig. 10, may for instance be obtained by epitaxial regrowth and coalescence after the formation of the PhC structure. While such a growth mode is challenging, the resulting structure would be advantageous for current injection: a *p*-electrode can be formed in the coalesced material, thus circumventing the usual difficulty of contacting the surface of the PhC. Thus, we obtain a photonic structure which keeps some properties of a PhC membrane (such as a vertically-localized mode with band gaps, which collects most of the light emission) but is easy to inject, in contrast to usual membranes. Such a structure may be considered for a PhC-based laser: current injection is easy, the mode is naturally confined vertically in the low-index region and its in-plane dispersion can be tailored through the parameters of the PhC.

Acknowledgments

This work was sponsored in part by the Department of Energy.

#85052 - $15.00 USD Received 9 Jul 2007; revised 26 Oct 2007; accepted 26 Oct 2007; published 18 Dec 2007